Phys. Status Solidi B **247**, No. 7, 1713–1716 (2010) / **DOI** 10.1002/pssb.200983650

physica status solidi b
www.pss-b.com
basic solid state physics

# A conductivity-based selective etching for next generation GaN devices

**Yu Zhang[1], Sang-Wan Ryu[2], Chris Yerino[1], Benjamin Leung[1], Qian Sun[1], Qinghai Song[3], Hui Cao[3], and Jung Han[*,1]**

[1] Department of Electrical Engineering, Yale University, New Haven, CT 06520, USA
[2] Department of Physics, Chonnam National University, Gwangju 500-757, Korea
[3] Department of Applied Physics, Yale University, New Haven, CT 06520, USA

Received 26 October 2009, accepted 6 November 2009
Published online 2 June 2010

**Keywords** III–V semiconductors, conductivity, electrochemical etching, microelectromechanical devices

[*] Corresponding author: e-mail jung.han@yale.edu, Phone: +01 203 432 7567, Fax: +01 203 432 7769

Electrochemical etching having large selectivity based on the conductivity of n-type GaN was investigated to demonstrate the feasibility of novel optical and microelectromechanical system devices. The electrochemical etching exhibited two regimes with different etching characteristics, i.e., nanoporous and electropolishing, depending on the doping concentration and applied voltage. For photonic applications, GaN microdisks and distributed Bragg reflectors were fabricated where optical index contrast can be achieved by selective etching or nanoporous formation of GaN. Stimulated emission of GaN microdisk was observed under pulsed optical pumping. In addition, a GaN cantilever was formed and its resonance frequency was measured at ~120 kHz.



**1 Introduction** The importance of GaN devices in display, data storage, and lighting applications is clearly established by now. In a more forward-looking manner, one may rightly ask about new opportunities the wide bandgap III-nitride family could offer, and new dimensions one could introduce to complement existing technologies. Over past two decades the epitaxy of GaN has been much explored while a flexible wet etching procedure is still to be desired. Due to its known chemical inertness, wet etching of Ga-polar GaN at room temperature can only be done through photoelectrochemical etching method [1] where photoexcited holes as minority carriers mediate an oxidation-etching mechanism [2]. This procedure has been incorporated into a selective etching technique with a combination of epitaxial heterostructures (InGaN/GaN) and bandgap selective photoexcitation [3]. As modern photonic and electromechanical devices call for etching processes with improved controllability, a few groups have utilized the epitaxy of "GaN-compatible" layers, that have sufficiently different chemical compositions and are more amenable to wet-etching. Two of such GaN-compatible layers are AlInN [4] and CrN [5], and there have been already interesting demonstrations. One of us reported recently [6] that a heavily doped ($n > 1 \times 10^{18}\,\mathrm{cm}^{-3}$) GaN can be selectively removed by an electrochemical (EC) etching with oxalic acid, a procedure often used in the anodic formation of porous aluminum oxide [7]. Distinct advantages of using n-GaN as the "sacrificial layer" for etching include (1) complete lattice matching to conventional GaN structures with negligible degradation in microstructure or morphology, (2) complete freedom in thickness design toward 1D, 2D, and 3D photonic-electronic-mechanical structures, and (3) the possibility of tuning the etching pathways at microscale through conductivity, bias, and solution, thus offering a new technique in crafting (i.e., etching, undercutting, and texturing) GaN. In this paper we report a mechanistic study of this EC etching to selectively remove conducting n-type GaN layers. We also present a few proof-of-concept demonstrations of photonic and microelectromechanical system (MEMS) device structures facilitated by this new method of etching.

**2 Experimental details** The EC etching was carried out in a setup schematically shown in Fig. 1. Oxalic acid was used as an electrolyte at room temperature with constant magnetic stirring. An indium-contacted GaN sample and a platinum wire were used as the anode and cathode, respectively. Constant voltage was applied to the sample and the resulting current increase was monitored. A

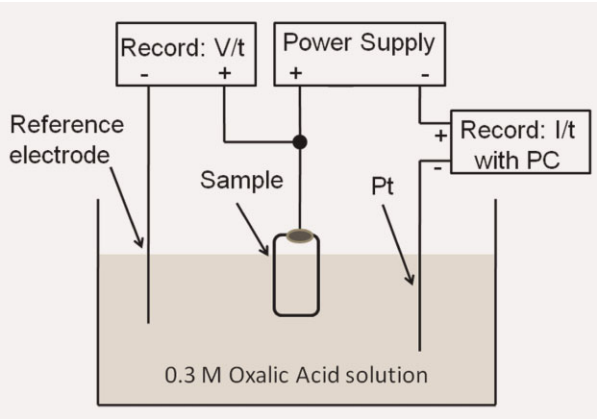


**Figure 1** The schematic of the EC etching setup.

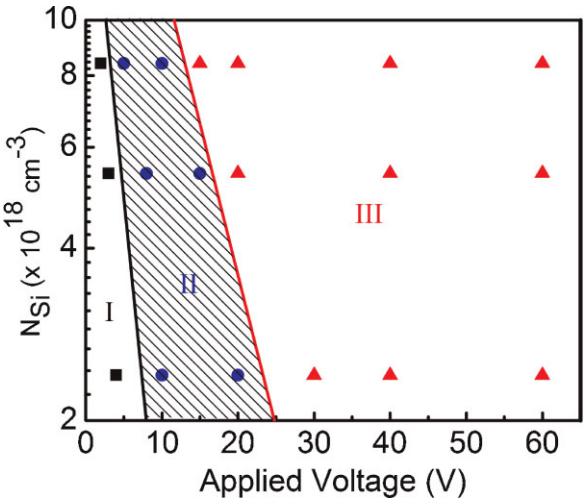


**Figure 2** (online color at: www.pss-b.com) Different etching characteristics related to the applied voltage and Si doping concentration ($N_{Si}$) of GaN. The symbols represent: ■ No etching (I), ● porous etching with varying porosity (II), and ▲ complete removal or electropolishing etching (III).

reference electrode (Ag/AgCl) was employed and it was determined that no measurable potential difference between the reference and anode electrodes existed. After the EC etching, samples were rinsed in deionized water, methanol, and pentane, sequentially to minimize surface tension in the final drying process.

Due to the unique conductivity-based etching selectivity, we prepared multi-layer GaN samples with contrasting conductivities where $n^+$-GaN served as a sacrificial layer. Standard two-step growth procedure was performed [8, 9] with 1-μm thick undoped GaN followed by either single or multiple n-GaN layers (doping from $10^{18}$ to $10^{19}$ $cm^{-3}$) before capping with 1–2 μm of undoped GaN layer. The Si-doping concentrations of n-GaN were verified by Hall measurement.

Etching morphology was studied by a field emission scanning electron microscope (SEM). Atomic force microscopy (AFM) was used to determine the roughness of as-grown and etched GaN surfaces. For optical pumping experiments, a Nd:YAG laser (pulse width = 32 ps, center wavelength = 355 nm, pulse repetition rate = 10 Hz) was focused through a microscope objective (25×, NA = 0.5) directed normal to the sample surface. Light emission spectra were collected by the same microscope objective and dispersed through a 0.75 m spectrometer (JOBIN-YVON-SPEX TRIAX 550) into a CCD detector (SpectrumONE). A commercial AFM (Veeco Nanoscope IIIa) in tapping mode was used to measure the resonance of fabricated cantilevers. The cantilevers were mounted on the AFM tip holder, and the laser beam was focused on the cantilever tip. The vibrational behavior was studied by mechanically driving the cantilever through the AFM piezo-stage over a range of frequencies. The deflection of the cantilever was measured using a laser spot reflected from the top surface of the cantilever into an array of photodiodes.

**3 Results and discussion** Figure 2 summarizes the "phase diagram" of this EC etching for GaN. The observed etching morphology is correlated with the applied voltage (5–60 V) and n-type GaN doping ($10^{18}$–$10^{19}$ $cm^{-3}$). The concentration of the oxalic acid was varied between 0.03 and 0.3 M with no strong dependence observed; 0.3 M was therefore used for all the following experiments. Three regions are identified based on SEM imaging, including no etching (region I), formation of porous GaN (II), and complete layer removal or electropolishing (III), with increasing conductivity or applied voltage.

Over the past three decades, tremendous efforts have been devoted to the mechanistic study of EC etching of silicon [10–13]. It is generally recognized that EC etching of silicon involves three essential components, all having complex natures at nano- and meso-scales. (i) The EC reactions at the electrode/electrolyte interface, which is further differentiated as either a space-charge-layer/Helmholtz-layer (HL) interface, or an oxide-layer/HL interface. (ii) The transport of reactants, mobile carriers, and ions into and across various layers that can pose rate-limiting conditions for reactions in (i). (iii) The spatial and temporal distribution of reactants, ions, and carriers that lead to inhomogeneous and porous morphology. While the details of GaN electrochemistry in oxalic acid has not been established and is beyond the scope of the present study, we note that the observation of three distinct regions is in qualitative agreement with most of the porous silicon works [11, 12], indicating that physical chemistry such as majority and minority carrier transport, ion diffusion, and reactant transport in electrolyte are possibly responsible for the formation of porous GaN. As the focus of the present work is on the utilitarian demonstration, we would refer the existing body of porous-silicon literature as an excellent guide for future attempt to resolve the mechanistic details.

In spite of the observed similarity in three-zone etching (Fig. 2) between GaN and Si, we note that the majority of porous-silicon works were carried out on bulk substrates in a

planar manner with etching direction perpendicular to the wafer surface. The properties of nanoporous GaN formed by the EC etching in a planar configuration will be reported elsewhere. In the following we describe a few proof-of-concept demonstrations of photonic and MEMS structures enabled by the lateral etching where a designed doping profile through epitaxy leads to useful two- and three-dimensional devices.

Figure 3(a) shows an array of GaN microdisks (diameter = 10 μm, thickness = 1 μm). The disk perimeter was defined through a Chlorine-based reactive ion etching (~2.1 μm deep), followed by the lateral EC etching of $n^+$-GaN ($n \sim 8 \times 10^{18}\,cm^{-3}$) at applied voltage of 20 V (region III in Fig. 1). We note that uniform undercut etching can be maintained over hundreds of micrometers. Optical pumping was performed on the microdisks; spectral properties from a particular disk with a 20-μm diameter are shown in Fig. 3(b). From the emission spectrum, the presence of optical microcavity modes is clearly discernable from regularly spaced spectral lines having linewidths much less than that from GaN near bandedge emission (~5 nm). The wavelength spacing between major modes are around 1 nm, and it agrees well with theoretically predicted mode spacing of whispering gallery modes [14]. The quality factor of the cavity is low and is at present limited by the roughness (~10 nm) of microdisk sidewall due to inhomogenous etching of the $SiO_2$ mask during the RIE process. We have also examined both the Ga-polar and N-polar surfaces of GaN created by the undercut etching; roughness of ~5 and ~10 nm over $10 \times 10\,\mu m^2$ was determined by AFM, respectively. Plot of measured optical intensity as a function of excitation level exhibits a clear threshold behavior and suggests the presence of stimulated emission. The relative high threshold power density is attributed to the absence of carrier confinement (i.e., InGaN quantum wells) in these initial structures, the self-absorption from the GaN microdisk beyond the laser excitation volume, and the optical losses from the sidewall scattering.

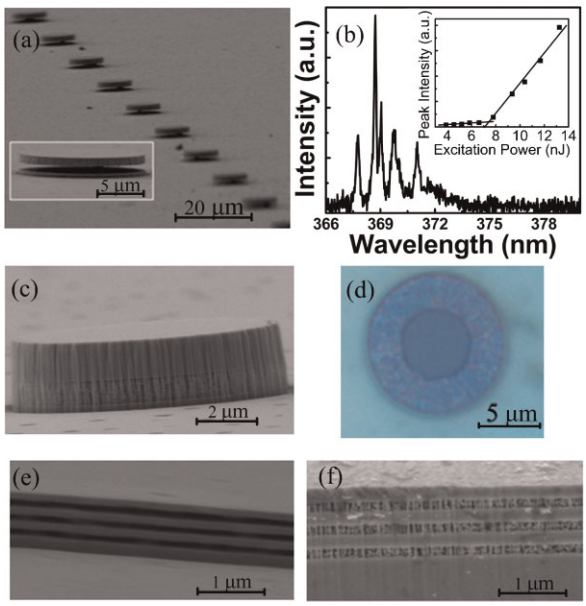


**Figure 3** (online color at: www.pss-b.com) (a) GaN microdisk array prepared by selective lateral undercut etching. (b) Light emission spectrum from an optically-pumped GaN disk after threshold. The inset shows the emission intensity versus excitation power. (c) SEM and (d) optical microscope image of the GaN microdisk with a nanoporous layer. SEM images of (e) GaN/air, and (f) GaN/porous-GaN DBRs.

Performing EC etching on the same pattern but at a reduced voltage (region II), we can explore a new type of GaN microcavity where the porous GaN layer contiguous to the undoped GaN serves as a new nitride layer with a reduced index of refraction, as shown in Fig. 3(c). Its capability of modulating the reflection of light is shown from the Nomarski optical microscope image showing contrast between the un-etched central circle and the nanoporous layered outer ring as in Fig. 3(d). One may consider the porous GaN to be a low index continuous layer able to provide optical waveguiding. It is especially attractive due to its mechanical robustness and possible electrical conductivity.

Figure 3(e) and (f) shows our attempt to build multilayer GaN/air and GaN/porous-GaN structures for photonic applications. In this preliminary study we show that air gaps and nanoporous GaN down to a quarter of wavelength (0.1–0.2 μm) can be reliably achieved. Further reduction of the sacrificial n-GaN layer, however, leads to reduced undercut etching rate due to difficulties in reactant (fluid) transport in sub-100 nm region. Additionally, the interface abruptness tends to decline in sub-100 nm layer as a result of non-planar electric field distributions during the EC etching. These problems can conceivably be overcome with innovative doping procedures to tighten the spatial distribution. Compared to previous reports of distributed Bragg reflectors (DBR) from AlGaN/GaN [15], GaN/air [16], or AlInN/GaN [17] systems, the GaN/porous-GaN DBRs has a few advantages such as the absence of lattice strain, a relative simplicity in layer growth, possibility of current injection through mirrors, good mechanical robustness, and a tunable index of refraction. We believe the nanoporous GaN could provide new design freedom in light extraction and photonic engineering.

Finally, we present another utility of EC etching in forming a GaN cantilever device through undercut etching in Fig. 4(a). The relative large dimension of the cantilever (100 μm × 10 μm) reflects the particular mask employed in the initial study and the intention to demonstrate deep undercut on the spatial order of 10–50 μm; cantilevers at the nanometer scale [18] can in principle be made in a similar way. Mechanical resonance of the cantilever studied in an AFM setup is shown in Fig. 4(b). The center of multiple resonance peaks at around 120 kHz agrees well with the predicated value based on the following equation [19]

$$f = \frac{(1.875)^2 t}{2\pi l^2}\sqrt{\frac{E}{12\rho}}, \qquad (1)$$

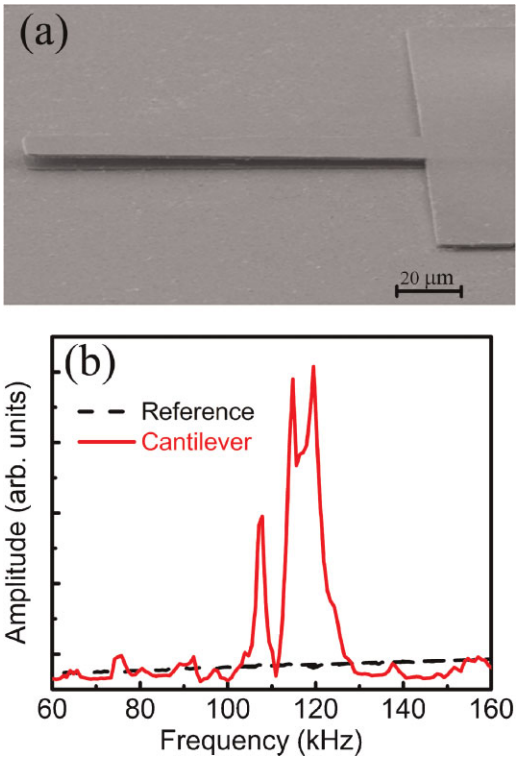


**Figure 4** (online color at: www.pss-b.com) (a) SEM image of a GaN cantilever prepared by the EC etching. (b) Spectral response of a GaN cantilever compared with a reference spectrum. The reference was obtained at un-etched wafer surface.

where $t$, $l$, $E$, and $\rho$ are the thickness (1 μm), the length (100 μm), the Young's modulus (295–390 GPa) [18], and the mass density (6.15 g/cm$^3$) of a GaN cantilever, respectively. The presence of multiple peaks might be due to the stray mechanical coupling during the acoustic excitation of cantilever holder [20].

**4 Conclusion** In summary, we studied the conductivity based selective etching of GaN at room temperature. Three regions are identified including no etching region, porous GaN formation region, and the complete removal or electropolishing region with increasing conductivity or applied voltage, which provides flexibility for the fabrication of GaN devices. Based on this etching technique, a few photonic applications (microdisks and DBRs) and a GaN cantilever were demonstrated. The simplicity of EC etching and its compatibility with conventional GaN structures allow us to anticipate a variety of useful device applications in the future.

**Acknowledgements** This work was partially supported by the US Department of Energy under Contract DE-FC26-07NT43227. Mr. Yu Zhang acknowledges the support from China Scholarship Council (CSC).

## References

[1] M. S. Minsky, M. White, and E. L. Hu, Appl. Phys. Lett. **68**, 1531 (1996).
[2] T. Rotter, D. Mistele, J. Stemmer, F. Fedler, J. Aderhold, J. Graul, V. Schwegler, C. Kirchner, M. Kamp, and M. Heuken, Appl. Phys. Lett. **76**, 3923 (2000).
[3] R. Stonas, T. Margalith, S. P. DenBaars, L. A. Coldren, and E. L. Hu, Appl. Phys. Lett. **78**, 1945 (2001).
[4] J. Dorsaz, H.-J. Bühlmann, J.-F. Carlin, N. Grandjean, and H. Ilegems, Appl. Phys. Lett. **87**, 072102 (2005).
[5] S. W. Lee, J.-S. Ha, H.-J. Lee, H.-J. Lee, H. Goto, T. Hanada, T. Goto, K. Fujii, M. W. Cho, and T. Yao, Appl. Phys. Lett. **94**, 082105 (2009).
[6] J. Park, K. W. Song, S.-R. Jeon, J. H. Baek, and S.-W. Ryu, Appl. Phys. Lett. **94**, 221907 (2009).
[7] H. Masuda and K. Fukuda, Science **268**, 1466 (1995).
[8] J. Han, T.-B. Ng, R. M. Biefield, M. H. Crawford, and D. M. Follstaedt, Appl. Phys. Lett. **71**, 3114 (1997).
[9] Q. Sun, Y. S. Cho, I.-H. Lee, J. Han, B. H. Kong, and H. K. Cho, Appl. Phys. Lett. **93**, 131912 (2008).
[10] M. I. J. Beale, J. D. Benjamin, M. J. Uren, N. G. Chew, and A. G. Cullis, J. Cryst. Growth **73**, 622 (1985).
[11] B. Hamilton, Semicond. Sci. Technol. **10**, 1187 (1995).
[12] X. G. Zhang, J. Electrochem. Soc. **151**, C69 (2004).
[13] V. Lehmann and U. Gosele, Appl. Phys. Lett. **58**, 856 (1991).
[14] E. D. Haberer, R. Sharma, C. Meier, A. R. Stonas, S. Nakamura, S. P. DenBaars, and E. L. Hu, Appl. Phys. Lett. **85**, 5179 (2004).
[15] K. E. Waldrip, J. Han, J. J. Figiel, H. Zhou, E. Makarona, and A. V. Nurmikko, Appl. Phys. Lett. **78**, 3205 (2001).
[16] R. Sharma, E. D. Haberer, C. Meier, E. L. Hu, and S. Nakamura, Appl. Phys. Lett. **87**, 51107 (2005).
[17] J.-F. Carlin and M. Ilegems, Appl. Phys. Lett. **83**, 668 (2003).
[18] T. Henry, K. Kim, Z. Y. Ren, C. Yerino, J. Han, and H. Tang, Nano Lett. **7**, 3315 (2007).
[19] L. Meirovich, Element of Vibration Analysis (McGraw-Hill, New York, 1986).
[20] C. Carrasco, P. Ares, P. J. de Pablo, and J. Gómez-Herrero, Rev. Sci. Instrum. **79**, 126106 (2008).

 